JACS
JOURNAL OF THE AMERICAN CHEMICAL SOCIETY

ARTICLE

pubs.acs.org/JACS

Controlling Ion Motion in Polymer Light-Emitting Diodes Containing Conjugated Polyelectrolyte Electron Injection Layers

Andres Garcia,[†] Ronald C. Bakus II,[†] Peter Zalar,[†] Corey V. Hoven,[‡] Jacek Z. Brzezinski,[†] and Thuc-Quyen Nguyen[†,*]

Center for Polymers and Organic Solids, [†]Department of Chemistry & Biochemistry, and [‡]Materials Department, University of California, Santa Barbara, California 93106, United States

Supporting Information

ABSTRACT: The properties and function of an anionic conjugated polyelectrolyte (CPE)-containing ion-conducting polyethylene oxide pendant ($PF_{PEO}CO_2Na$) as electron injection layers (EILs) in polymer light-emitting diodes (PLEDs) are investigated. A primary goal was to design a CPE structure that would enable acceleration of the device temporal response through facilitation of ion motion. Pristine PLEDs containing $PF_{PEO}CO_2Na$ exhibit luminance response times on the order of tenths of seconds. This delay is attributed to the formation of ordered structures within the CPE film, as observed by atomic force microscopy. Complementary evidence is provided by electron transport measurements. The ordered structures are believed to slow ion migration within the CPE EIL and hence result in a longer temporal response time. It is possible to accelerate the response by a combination of thermal and voltage treatments that "lock" ions within the interfaces adjacent to $PF_{PEO}CO_2Na$. PLED devices with luminance response times of microseconds, a 10^5 fold enhancement, can therefore be achieved. Faster luminance response time opens up the application of PLEDs with CPE layers in display technologies.

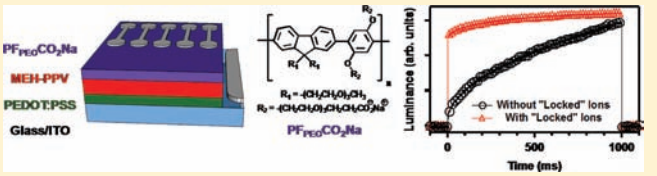

INTRODUCTION

Polymer light-emitting diodes (PLEDs)[1] composed of conjugated polymer semiconductors are an attractive emerging technology with potential advantageous features unavailable to inorganic counterparts, such as mechanical flexibility and solution processability. Charge injection plays a vital role in the device operation and performance. Balanced injection and transport of holes and electrons are necessary to increase the probability of hole/electron recombination and thereby increase light output. PLED devices can be fabricated with stable high work function anodes leading to little or no hole injection barriers; however, the use of stable high work function cathodes normally leads to devices with large electron injection barriers. Therefore, environmentally unstable low work function metals that require device encapsulation, such as barium and calcium,[2] or devices with multilayer structures,[3] are required.

Conjugated polyelectrolytes (CPE) containing a π-delocalized backbone and pendant ionic functionalities have recently received attention due to their effective function as electron injection layers (EILs) in PLEDs,[4] allowing the use of stable high work function metal cathodes such as Al, Au, and Ag.[4b] CPEs are soluble in polar solvents, thus allowing the fabrication of multilayer PLEDs using solution processing techniques, such as spin-coating and printing, by altering the solvent polarity of each succeeding layer, including the metal cathode,[4f] with no interfacial mixing.[5] The operating mechanism for the reduction of electron injection barriers is believed to be a combination of the formation of permanent interfacial dipoles between the cathode and the CPE,[4a,6] and ion migration under an applied electric field, leading to redistribution of the internal field within the CPE EIL.[7] Although the performance of PLEDs with CPE EILs/Al cathodes are comparable to devices with Ba cathodes having no electron injection barrier, the devices can exhibit long turn-on times attributed to slow ion migration.[7] Luminance response times in the order of seconds can be observed in PLEDs with CPE EILs, thus hindering application in display technologies. Thus, it is important to tune the chemical structure of CPE EIL to facilitate ion migration and hence improve the luminance response time.

This work focuses on the control of ion motion to improve the device response time by using CPE EILs with poly(ethylene oxide), PEO, unit. In this contribution, an anionic CPE ($PF_{PEO}CO_2Na$ in Scheme 1) containing substituents derived from PEO is investigated as an EIL in test bed PLEDs containing poly(2-methoxy-5-(2′-ethylhexyloxy)-1,4-phenylene vinylene) (MEH-PPV) as the emissive layer. PEO units have been shown to facilitate ion transport leading to increased ionic conductivities[8] and have been implemented in light-emitting electrochemical cells (LECs)[9] and in solid-state batteries.[10] Thus, PEO units were incorporated into the side groups in hope of facilitating ion motion and presumably reducing the luminance response time. In contrast to what has been observed in LECs, the use of $PF_{PEO}CO_2Na$ as EILs in PLEDs leads to longer luminance response times than other CPE EILs with alkyl substituents. However, the response times can be reduced

Received: July 15, 2010
Published: February 7, 2011

dx.doi.org/10.1021/ja106268w | J. Am. Chem. Soc. 2011, 133, 2492–2498

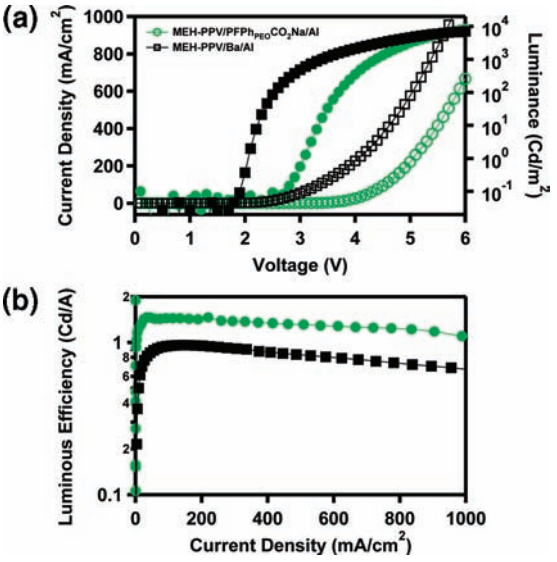

Figure 1. (a) J versus V (open symbols), L versus V (solid symbols), and (b) LE versus J plots of ITO/PEDOT:PSS/MEH-PPV/$PF_{PEO}CO_2Na$/Al (green circles) and ITO/PEDOT:PSS/MEH-PPV/Ba/Al (black squares) devices.

substantially from seconds to microseconds (μs) using a combination of thermal annealing and applied bias treatment to control the distribution of ions within the $PF_{PEO}CO_2Na$ layer.

EXPERIMENTAL SECTION

$PF_{PEO}CO_2Na$ was synthesized according to a previous reported procedure.[11] Differential scanning calorimeter (DSC) characterization was performed on a TA Instrument Q20 calorimeter with aluminum DSC pans. Samples were prescanned to remove any residual volatiles, and the second cycle of the DSC scan is reported. Film morphology and film thicknesses were measured by atomic force microscopy (AFM) using a commercial scanning probe microscope (MultiMode with a Nanoscope Controller IIIa, Veeco Inc.). All scanning probe measurements were performed under a dry N_2 atmosphere. Silicon probes with a spring constant of ~5 N/m and a resonant frequency of ~75 kHz (Budget Sensors) were used for tapping AFM measurements. Films thicknesses were controlled by varying the spin speed and solution concentration.

For device fabrication, indium tin oxide (ITO) substrates (Thin Film Devices, Inc.) were cleaned by successive rinsing and ultrasonic treatment in water, acetone, and isopropyl alcohol and then drying in an oven for 1 h. The substrates were treated with UV/O_3 prior to polymer solution deposition. PLED devices with a ITO/PEDOT:PSS/MEH-PPV/$PF_{PEO}CO_2Na$/Al architecture were fabricated by first spin-coating a ~100 nm PEDOT:PSS (Baytron P 4083, Bayer AG.) onto a clean ITO-coated glass followed by drying at 150 °C for 1 h. PEDOT:PSS is poly(3,4-ethylenedioxythiophene):poly(styrenesulfonate). Subsequently, a 60 nm MEH-PPV emissive layer was deposited from a 0.5% g/mL toluene solution at 1500 rpm. The $PF_{PEO}CO_2Na$ EIL was then spin-coated from a 0.5% g/mL 3:7 (v:v) water:methanol solution at 3000 rpm yielding a ~20 nm film. The films were then dried under a vacuum (10^{-6} Torr) for 12 h before thermal evaporation of the Al cathode electrodes. Reference devices ITO/PEDOT:PSS/MEH-PPV/Ba/Al without an electron injection barrier between the cathode electrode and the MEH-PPV emissive layer were also fabricated for comparison. All fabrication and testing were performed inside a N_2 atmosphere glovebox.

For PLED temporal response measurements, a +3.2 V square voltage pulse was applied to devices by using a Keithley 4200 pulse generator.

Scheme 1. Chemical Structures of $PF_{PEO}CO_2Na$ and MEH-PPV, Energy Levels, and the PLED Device Architecture

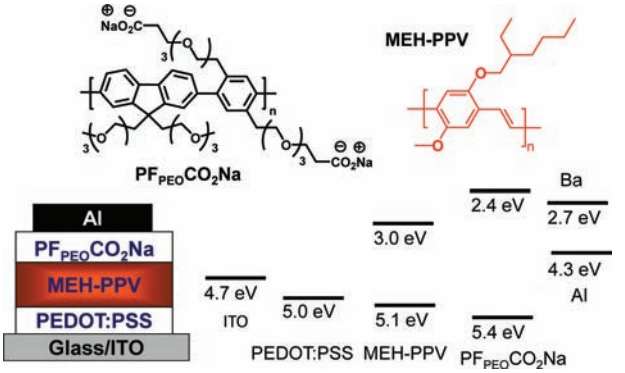

The luminance signal collected from a photodetector (Thorlabs, Inc.) was measured with a current preamplifier (Stanford Research Systems, model SR570) and a digital oscilloscope (Tektronix) with a 20 μs resolution. Measurements were preformed with a single voltage pulse, necessary for accurate luminance response time measurements since continual application of voltage pulses leads to faster temporal responses after each succeeding pulse in all CPE devices due to slow ion relaxation.

For electron transport measurements, electron-only diodes were fabricated by spin-coating (900 rpm for 60 s) relatively thick $PF_{PEO}CO_2Na$ films (120 nm) onto thermally evaporated Al-coated glass substrates, followed by thermal evaporation of Ba (~5 nm) and Al (~100 nm) using a shadow mask. Electrical measurements were performed with stepped-pulse voltage scans to reduce ion motion, which can lead to modification of injection barriers in these mixed electronic/ionic charge conducting systems.[4e,12] Voltage measurements were performed with 500 ms off-times and 5 ms on-times for step pulsed voltage scans.

Electroabsorption experiments were done on the electroabsorption spectrometer using a Keithley 236 source measure unit and a SRS DS345 function generator to provide the d.c. and a.c. electric fields to the device. The ac bias used was 1.5 $V_{peak\text{-}to\text{-}peak}$ at 1500 Hz. A 75 W zenon arc-lamp is used as the light source. The details of the experimental setup has been published elsewhere.[13]

RESULTS AND DISCUSSION

Scheme 1 shows the chemical structures of $PF_{PEO}CO_2Na$ and MEH-PPV, together with the PLED configuration. $PF_{PEO}CO_2Na$ consists of a polyfluorene-phenylene-conjugated polymer backbone, tethered PEO chains with carboxylate substitutents, and sodium counterions, a combination that was anticipated to enhance migration of the mobile countercations. The PLED structure used in this study to test the function of $PF_{PEO}CO_2Na$ is ITO/PEDOT:PSS/MEH-PPV/$PF_{PEO}CO_2Na$/Al. MEH-PPV was chosen as the electroluminescent layer because of its extensive previous characterization in PLED devices.[14] Reference devices without an electron injection barrier (ITO/PEDOT:PSS/MEH-PPV/Ba/Al) were also fabricated for comparison. These devices have no electron injection barrier at the Ba/MEH-PPV interface because of a work function energy of Ba (~2.7 eV) lower than the lowest unoccupied molecular orbital (LUMO) energy of MEH-PPV (~3.0 eV).[15]

The current density, luminance versus voltage ($J-V$ and $L-V$), and luminance efficiency versus current density (LE$-J$) characteristics of the PLEDs fabricated in our studies are shown

dx.doi.org/10.1021/ja106268w |J. Am. Chem. Soc. 2011, 133, 2492–2498

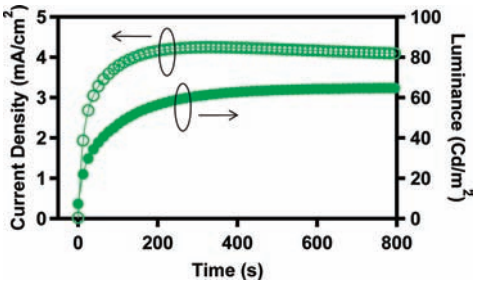

Figure 2. Temporal response of J and L for a ITO/PEDOT:PSS/MEH-PPV/$PF_{PEO}CO_2Na$/Al device operated with a +3.2 V constant applied bias.

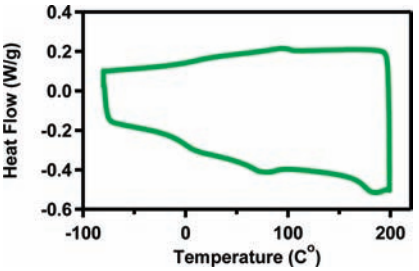

Figure 3. DSC plot of $PF_{PEO}CO_2Na$.

in Figure 1. Devices with $PF_{PEO}CO_2Na$ and Al exhibit excellent performance, as indicated by a low luminance turn-on voltage (3 V at 1 Cd/m^2), high luminance at low bias (9000 Cd/m^2 at 6 V), and luminance efficiencies higher than that of the reference ITO/PEDOT:PSS/MEH-PPV/Ba/Al device (1.4 Cd/A versus 0.9 Cd/A at 200 mA/cm^2). The device performance of $PF_{PEO}CO_2Na$ is comparable to other efficient CPE EILs,[7] indicating its effective function in PLEDs.

Despite the effective overall function of $PF_{PEO}CO_2Na$ as an EIL, the devices exhibit relatively long luminance response times, which we define as the time when the luminance reaches 50% of its maximum value. From time response measurements obtained by operating devices at a constant +3.2 V (Figure 2), and monitoring J and L, a luminance response time of ~46 s was calculated, much longer than observed in other CPEs (~9 s) under similar luminance output and EIL thickness (~20 nm).[5b] The long response time observed in PLEDs with CPE EILs is believed to be due to slow ion migration within the CPE EIL.[7b,5c] The longer luminance response time observed here with a $PF_{PEO}CO_2Na$ EIL indicates a further reduction in ion migration, which was unanticipated on the basis of extensive precedent of increased ionic conductivity promoted by PEO.[8]

PEO units are known to substantially increase ion conductivity of positive charge ions in films by a combination of ion diffusion along the chains and ion hopping between chains.[16] Critical to this process is the phase of the material. Films must be in a liquid/rubbery state above the glass transition temperature (T_g) of the PEO chains, allowing the flexibility and motion of chains to facilitate ion movement between transport sites.[16] DSC measurements of $PF_{PEO}CO_2Na$ powders show several thermal transitions. Scans performed at a rate of 5 °C/min from −80 °C to +200 °C and back to −80 °C show a glass transition at −10 °C, followed by two endothermic peaks at 75 and 180 °C (Figure 3). These signals approximately correspond to the glass transition (~−65 °C) and melting transitions of pure (~60 °C) and ion complex (~170 °C) of PEO chains reported in the literature.[17] Since the PLEDs described here operate at room temperature (or higher), which is above the T_g of $PF_{PEO}CO_2Na$, faster ion motion should be observed. However, the device response time is longer. It is possible that spin-casting $PF_{PEO}CO_2Na$ from the polar water:methanol medium may lead to films with high levels of crystallinity or ordered structures in which ion migration is inhibited.

To investigate the possible contribution of the solid-state structure in $PF_{PEO}CO_2Na$ films on the relatively long luminance response time observed, the film morphology was investigated by atomic force microscopy (AFM) as a function of processing history. These studies were motivated by previous reports on how thermal treatment[18] and solution concentration[19] can be used to enhance order in polymer films. Figure 4 shows topographic and phase images of the as-cast and annealed $PF_{PEO}CO_2Na$ surfaces collected from areas between the Al cathodes. Figure 4a and 4b shows topographic images of as-cast and annealed $PF_{PEO}CO_2Na$ surfaces containing circular features (bright regions). The film thickness of the CPE layer atop the MEH-PPV layer is around 20 nm as measured by AFM. There was no significant change in the film thickness upon thermal annealing. Annealing the device at 80 °C above the melting temperature (T_m) of $PF_{PEO}CO_2Na$ and then cooling the device to room temperature or increasing the $PF_{PEO}CO_2Na$ concentration leads to a larger number of these features. We assign these large features to aggregated particles, which can be confirmed by the phase images. Phase imaging detects different tip−sample interactions arising from different physical properties within a film such as amorphous and crystalline domains.[20] The phase images of $PF_{PEO}CO_2Na$ surfaces show different degrees of aggregation or order structures depending on processing conditions. The phase image of the as-cast $PF_{PEO}CO_2Na$ surface shows interpenetrating fiber-like nanostructures (Figure 4d). The phase contrast observed leads us to believe that the $PF_{PEO}CO_2Na$ surface consists of amorphous and ordered or crystalline domains. Upon thermal annealing, the ordered structures increase in size with most of the film surface covered with connected fiber-like nanostructures and large domains with substructures (Figure 4e). Thus, the AFM results confirm that the degree of film crystallinity increases by thermally annealing above the T_m determined by DSC followed by cooling to room temperature. Additional evidence of crystallization in $PF_{PEO}CO_2Na$ films is observed by casting films from higher concentration solutions. Films cast from 1.5% g/mL solutions exhibit longer fibers on the surface than that of films cast at the lower concentrations used for device fabrication (0.5% g/mL); see Figure 4c. The film thickness is around 120 nm. This observation agrees with previous reports that increasing solution concentration promotes polymer chain interactions leading to higher crystallinity in polymer films.[19]

To further support the high degree of order in $PF_{PEO}CO_2Na$ films, the electron mobility was measured. Ordered aggregation results in stronger electronic coupling between conjugated polymer chains, which is generally accepted to lead to higher charge carrier mobilities. Thus, the electron mobility of $PF_{PEO}CO_2Na$ was expected to be higher than those of less crystalline anionic CPEs without PEO units. Electron mobility measurements were performed using electron-only diodes[21] fabricated by sandwiching $PF_{PEO}CO_2Na$ films (120 nm) between an Al substrate and evaporated Ba/Al top electrodes. The relative low work function of the Al and Ba electrodes in comparison to the lowest unoccupied molecular orbital energy of $PF_{PEO}CO_2Na$

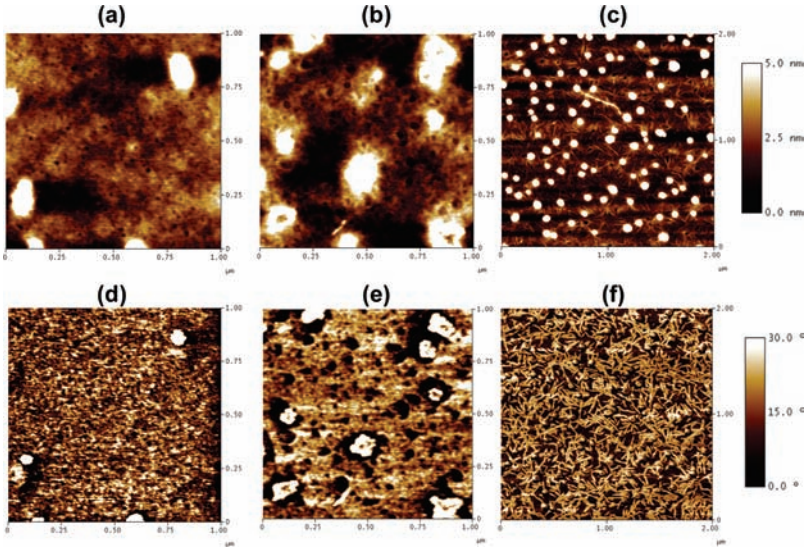

Figure 4. AFM topographic (a, b, and c) and phase (d, e, and f) images of $PF_{PEO}CO_2Na$ surface collected between Al electrodes (a, d) before and (b, e) after annealing at 80 °C and $PF_{PEO}CO_2Na$ film cast from a higher concentration (c, f). The size of images a, b, d, and e is 1 μm × 1 μm, and the size of images c and f is 2 μm × 2 μm.

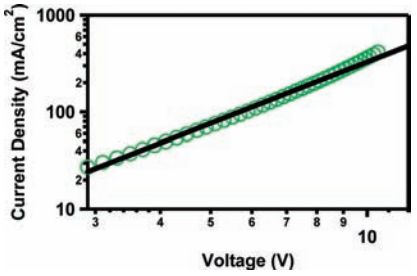

Figure 5. J versus V plot of $PF_{PEO}CO_2Na$ electron-only diodes with fitted line.

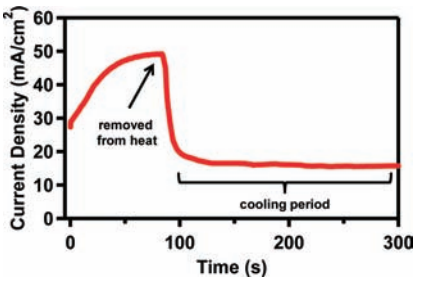

Figure 6. Current density versus time plot of the PLED during the ion "locking" procedure.

ensures electrons as the majority injected charge carriers. These measurements were performed with a high frequency stepped pulse voltage sweep at a frequency faster (5 ms) than ion migration (~0.1 s to 100 s)[9b,22] to reduce ion migration to the electrode interface in the CPE[4e,12] to form electrical double layers[23] that lead to light-emitting electrochemical behavior (LEC) in CPE films.[12,24] Figure 5 shows the $J-V$ plots of $PF_{PEO}CO_2Na$ electron-only devices and the fitted line to the space-charge-limited-current (SCLC) model from which electron mobility can be extracted.[12,21]

$$J = \frac{9}{8}\varepsilon_o\varepsilon_r\mu\frac{V^2}{L^3} \quad (1)$$

In eq 1, ε_o is the vacuum permittivity, ε_r is the relative dielectric constant of the film, μ is the mobility at a specified electric field, V is the applied voltage, and L is the thickness of the active layer. A good fit of the $J-V$ measurement and eq 1 was observed, and an electron mobility of 2.1×10^{-5} $cm^2/V\cdot s$ was extracted, approximately 2 orders of magnitude larger than the mobility of a similar anionic CPE without appended PEO substituents.[4e] The crystalline or ordered structures in $PF_{PEO}CO_2Na$ films induced by aggregation of the PEO substituents leads to the higher electron mobility. Crystallinity in ionic conducting polymers, however, is known to impede ion transport.[8,16a,17a,17d] Thus, these results provide a plausible explanation for the observed longer temporal response times of $PF_{PEO}CO_2Na$ devices.

To facilitate ion transport and accelerate the PLED response time, we first thermally annealed the device at temperatures above T_m, while applying a small bias ($V_{applied} < V_{ON}$) and then cooled the device rapidly while still under an applied bias to "freeze" or "lock" the ions at the $PF_{PEO}CO_2Na$/Al and MEH-PPV/$PF_{PEO}CO_2Na$ interfaces. Subsequent operation of the device requires minor or no further ion transport to the interfaces, hence leading to faster luminance temporal responses. The J of a PLED device during this procedure is shown in Figure 6. A +3.2 V bias was first applied to the device at 80 °C until a maximum J value was reached, an indication of ion accumulation at the interfaces, followed by rapid cooling to room temperature by removing the device under bias from the heating source.

The $J-V$, $L-V$, and LE$-J$ plots of the devices with and without the heat/bias treatment are shown in Figure 7. Both devices have similar L (10 000 Cd/m^2 and 6000 Cd/m^2) and LE (1.4 Cd/A and 1.2 Cd/A) values. However, the luminance turn-on voltage drops from 2.8 to 2.0 V in devices with heat and bias treatment (red triangles), possibly due to the presence of an interfacial dipole locked in the heat/bias treated device. The slight drop in L and LE values is attributed to the heat treatment, which may adversely affect the morphology and emission properties of the MEH-PPV layer.[14a]

dx.doi.org/10.1021/ja106268w | J. Am. Chem. Soc. 2011, 133, 2492–2498

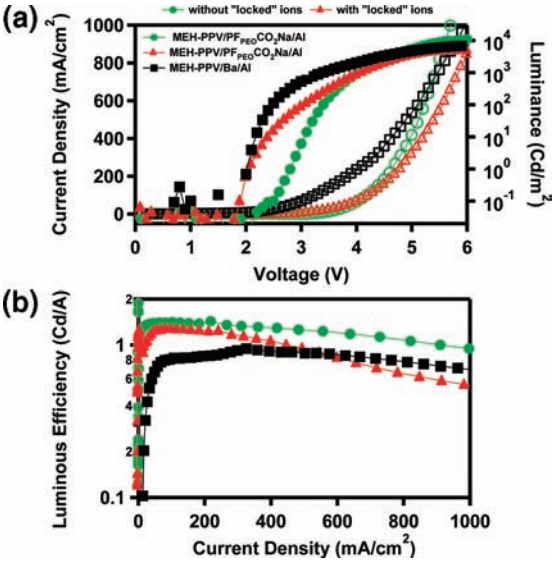

Figure 7. (a) J versus V (open symbols), L versus V (solid symbols) and (b) LE versus J plots of ITO/PEDOT:PSS/MEH-PPV/PF$_{PEO}$CO$_2$Na/Al with (red triangles) and without (green circles) "locked" ions and ITO/PEDOT:PSS/MEH-PPV/Ba/Al (black squares) reference devices.

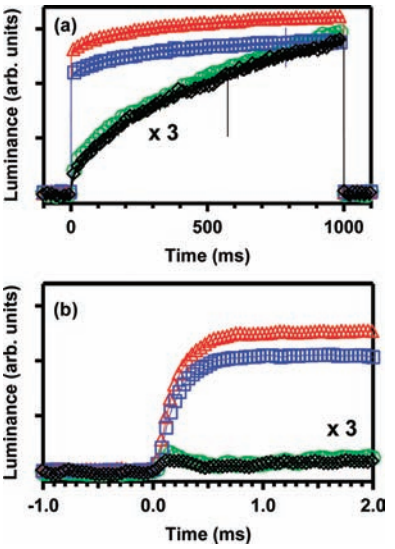

Figure 8. (a) Luminance temporal response measurements of ITO/PEDOT:PSS/MEH-PPV/PF$_{PEO}$CO$_2$Na/Al devices without "locked" ions (green circles) and with "locked" ions measured on the same day (red triangles), 1 week after fabrication (blue squares), and annealing without an applied bias (black diamonds). (b) Close-up of response measurements at shorter time scales.

Luminance versus time measurements of devices with (red triangles) and without (green circles) "locked" ions measured at +3.2 V shown in Figure 8 show a luminance response time of ~200 μs in devices with "locked" ions (red triangles), a greater than 10^5 fold enhancement in luminance response times relative to as-cast (~46 s) devices (Figure 8b). Annealing the devices at 40 and 60 °C while +3.2 V is applied also improves the response times to 300 ms and 9 s, respectively (Figure S1, Supporting Information). To confirm that the faster response time is due to the "locked" ions, we performed electroabsorption spectroscopy to probe the internal electric field of the ITO/PEDOT:PSS/MEH-PPV/PF$_{PEO}$CO$_2$Na/Al and the ITO/PEDOT:PSS/MEH-PPV/Al reference device. If ion motion takes place, the ions are then redistributed within the ETL to screen the electric field in the emitting layer at applied biases greater than the built-in field of the device.[13] The built-in voltages, defined as the voltage as which the electric field is zero, for the ITO/PEDOT:PSS/MEH-PPV/PF$_{PEO}$CO$_2$Na/Al and the reference device are very similar (1.46 and 1.39 V, respectively). Below voltages of 1.5 V, the EA signal varies linearly and crosses the x-intercept at 1.46 V. At voltages greater than 1.46 V, the electroabsorption signal remains ~0, confirming that the electric field in the emissive layer is screened. However, this is not the case for the reference device where the electroabsorption signal is negative at voltages greater than 1.39 V (Figure S2, Supporting Information). Thus, the faster response time is due to the "locked" ions.

The reversibility of these devices, important for long-term applications, was also studied. The performance of devices with "locked" ions remained unchanged after one week, exhibiting luminance response times similar to that from the initial conditions (Figure 8). Possibly, there is a large activation barrier for ions to move in crystalline PF$_{PEO}$CO$_2$Na film at room temperature. The long response time in devices was also found to be restored only upon annealing above T_m for over 20 min under no applied bias (black diamonds). Annealing the device again above T_m without an applied bias is believed to melt the crystalline domains, allowing ions to equilibrate back to a charge-compensating state homogenously distributed throughout the PF$_{PEO}$CO$_2$Na layer. This ion redistribution only takes place during the annealing process where the polymer is in the melt state.

CONCLUSION

An anionic CPE, PF$_{PEO}$CO$_2$Na, containing PEO substituents was investigated as an EIL in PLEDs in an effort to improve the luminance temporal response of devices, which is limited by the time it takes for ions to redistribute in response to the applied field. Surprisingly, a much longer response time of 46 s was observed. Thus, the presence of the ethylene oxide units on PF$_{PEO}$CO$_2$Na was found not to improve the luminance response times of as-cast PLEDs, despite previous precedent in LECs where PEO is mixed to better accommodate ion motion.[9] We have shown that PF$_{PEO}$CO$_2$Na exhibits crystalline or ordered structure in film, as observed by AFM and supported by electron transport measurements. This observation may originate from the complex structure of CPEs which consists of a rigid hydrophobic backbone and hydrophilic side groups. However, by taking advantage of the thermal properties of PF$_{PEO}$CO$_2$Na films in combination with an applied voltage treatment to "lock" ions at the EIL interfaces, the device turn-on time can be substantially reduced from 46 s to 200 μs. Hence, efficient multilayer solution-processable PLEDs with stable high work function cathodes and fast luminance response time can be achieved. The faster luminance temporal response opens the possibility of using CPE injection layers not only in lighting applications but in display technologies as well.

ASSOCIATED CONTENT

Supporting Information. Luminance temporal response measurements of devices without "locked" ions processed at different temperatures and the electroabsorption results. This material is available free of charge via the Internet at http://pubs.acs.org.

AUTHOR INFORMATION

Corresponding Author
quyen@chem.ucsb.edu

ACKNOWLEDGMENT

A.G. is supported by the NSF CAREER Award (DMR# 0547639). P.Z. and C.V.H. are supported by the DOE (DE-SC0002368). The authors thank the Camille Dreyfus Teacher Scholar Award, the National Science Foundation via Jackson State University, and the University of California, Santa Barbara (DMR0611539) for partially supporting this work. T.-Q.N. is an Alfred P. Sloan Foundation Research Fellow.

REFERENCES

(1) (a) Burroughes, J. H.; Bradley, D. D. C.; Brown, A. R.; Marks, R. N.; Mackay, K.; Friend, R. H.; Burns, P. L.; Holmes, A. B. *Nature* **1990**, *347*, 539. (b) Braun, D.; Heeger, A. J. *Appl. Phys. Lett.* **1991** *58*, 1982. (c) Friend, R. H.; Gymer, R. W.; Holmes, A. B.; Burrougnes, J. H.; Marks, R. N.; Taliani, C.; Bradley, D. D. C.; Dos Santos, D. A.; Brédas, J. L.; Lögdlund, M.; Salaneck, W. R. *Nature* **1999**, *397*, 121. (d) Bernius, M. T.; Inbasekaran, M.; O'Brien, J.; Wu, W. *Adv. Mater.* **2000**, *12*, 1737. (e) Sirringhaus, H.; Tessler, N.; Friend, R. H. *Science* **1998**, *280*, 1741.

(2) (a) Scott, J. C.; Kaufman, J. H.; Brock, P. J.; DiPietro, R.; Salem, J.; Goitia, J. A. *J. Appl. Phys.* **1996**, *79*, 2745. (b) Cao, Y.; Yu, G.; Parker, I. D.; Heeger, A. J. *J. Appl. Phys.* **2000**, *88*, 3618. (c) Bharathan, J. M.; Yang, Y. *J. Appl. Phys.* **1998**, *84*, 3207. (d) Brown, T. M.; Millard, I. S.; Lacey, D. J.; Butler, T.; Burrouhes, J. H.; Friend, R. H. *J. Appl. Phys.* **2003**, *93*, 6159.

(3) (a) Shen, Y. L.; Hosseini, A. R.; Wong, M. H.; Malliaras, G. G. *Chem. Phys. Chem.* **2004**, *5*, 16. (b) Chen, J. P.; Klaerner, G.; Lee, J. I.; Markiewicz, D.; Lee, V. Y.; Miller, R. D.; Scott, J. C. *Synth. Met.* **1999**, *107*, 129. (c) Vaeth, K. M.; Jensen, K. F. *Adv. Mater.* **1997**, *9*, 490.

(4) (a) Wu, H.; Huang, F.; Mo, Y.; Yang, W.; Wang, D.; Peng, J.; Cao, Y. *Adv. Mater.* **2004**, *16*, 1826. (b) Wu, H.; Huang, F.; Peng, J.; Cao, Y. *Org. Electron.* **2005**, *6*, 118. (c) Ma, W.; Iyer, P. K.; Gong, X.; Liu, B.; Moses, D.; Bazan, G. C.; Hegger, A. J. *Adv. Mater.* **2005**, *17*, 274. (d) Yang, R.; Wu, H.; Cao, Y.; Bazan, G. C. *J. Am. Chem. Soc.* **2006**, *128*, 14423. (e) Garcia, A.; Yang, R.; Jin, Y.; Walker, B.; Nguyen, T.-Q. *Appl. Phys. Lett.* **2007**, *91*, 153502. (f) Zeng, W.; Wu, H.; Zhang, C.; Fuang, F.; Peng, J.; Yang, W.; Cao, Y. *Adv. Mater.* **2007**, *19*, 810. (g) Hoven, C. V.; Garcia, A.; Bazan, G. C.; Nguyen, T.-Q. *Adv. Mater.* **2008**, *20*, 3793.

(5) (a) Steuerman, D. W.; Garcia, A.; Dante, M.; Yang, R.; Lofvander, J. P; Nguyen, T.-Q. *Adv. Mater.* **2008**, *20*, 528. (b) Wang, C.; Garcia, A.; Yan, H.; Sohn, K. E.; Hexemer, A.; Nguyen, T.-Q.; Bazan, G. C.; Kramer, D. J.; Ade, H. *J. Am. Chem. Soc.* **2009**, *131*, 12538. (c) Ade, H.; Wang, C.; Garcia, A.; Yang, H.; Sohn, K. E.; Hexemer, A.; Bazan, G. C.; Nguyen, T.-Q.; Kramer, E. J. *J. Polym. Sci., Part B: Polym. Phys.* **2009**, *47*, 1291.

(6) (a) Seo, J. H.; Nguyen, T.-Q. *J. Am. Chem. Soc.* **2008**, *130*, 10042. (b) Seo, J. H.; Yang, R.; Brzezinski, J. Z.; Walker, B.; Bazan, G. C.; Nguyen, T.-Q. *Adv. Mater.* **2009**, *21*, 1006.

(7) (a) Hoven, C.; Yang, R.; Garcia, A.; Heeger, A. J.; Nguyen, T.-Q.; Bazan, G. C. *J. Am. Chem. Soc.* **2007**, *129*, 10976. (b) Hoven, C.; Yang, R.; Garcia, A.; Crocett, V.; Heeger, A. J.; Bazan, G. C.; Nguyen, T.-Q. *Proc. Natl. Acad. Sci. U.S.A.* **2008**, *105*, 12730. (c) Hoven, C. V.; Peet, J.; Mikhailovsky, A.; Nguyen, T.-Q. *Appl. Phys. Lett.* **2009**, *94*, 033301.

(8) (a) MacCallum, J. R.; Vincent, C. A. *Polymer Electrolyte Reviews 2*; Elsevier: London, 1989. (b) Armand, M. B.; Chabango, J. M.; Duclot, M. J. *Fast Ion Transport in Solids*; North-Holland: New York, 1979, p 131.(c) Wright, P. V. *Br. Polym.* **1975**, *7*, 319. (d) Armand, M. B. *Annu. Rev. Mater. Sci.* **1986**, *16*, 245. (e) Kelly, I.; Owen, J. R.; Steele, B. C. H. *J. Electroanal. Chem.* **1984**, *168*, 467. (f) Gadjourova, Z.; Andreev, Y. G.; Tunstall, D. P.; Bruce, P. G. *Nature* **2001**, *412*, 520.

(9) (a) Pei, Q.; Yu, G.; Zang, C.; Yang, Y.; Heeger, A. J. *Science* **1995**, *269*, 1086. (b) Pei, Q.; Yang, Y.; Yu, G.; Zhang, C.; Heeger, A. J. *J. Am. Chem. Soc.* **1996**, *118*, 3922. (c) Yang, Y.; Pei, Q. *J. Appl. Phys.* **1997**, *81*, 3294. (d) Tach, S.; Holzer, L.; Wenzl, F. P.; Gao, J.; Winkler, B.; Dai, L.; Mau, A. W. H.; Sotgiu, R.; Sampietro, M.; Scherf, U.; Müllen, K.; Heeger, A. J.; Leising, G. *Synth. Met.* **1999**, *102*, 1046.

(10) (a) Angell, C. A.; Liu, C.; Sanchez, E. *Nature* **1993**, *362*, 137. (b) Croce, F.; Appetecchi, G. B.; Persi, L.; Scrosati, B. *Nature* **1998**, *394*, 456. (c) Nagasubramanian, G.; Attia, A. I.; Halpert, G. *Solid State Ionics* **1993**, *67*, 51. (d) Meyer, W. H. *Adv. Mater.* **1998**, *10*, 439. (e) Song, J. Y.; Wang, Y. Y.; Wan, C. C. *J. Power Sources* **1999**, *77*, 183.

(11) Wang, F.; Bazan, G. C. *J. Am. Chem. Soc.* **2006**, *128*, 15786.

(12) (a) Garcia, A.; Nguyen, T.-Q. *J. Phys. Chem. C* **2008**, *112*, 7054. (b) Elbing, M.; Garcia, A.; Urban, S.; Nguyen, T.-Q.; Bazan, G. C. *Macromolecules* **2008**, *41*, 9146.

(13) Hoven, C. V.; Peet, J.; Mikhailovsky, A.; Nguyen, T.-Q. *Appl. Phys. Lett.* **2009**, *94*, 033301.

(14) (a) Schwartz, B. J. *Annu. Rev. Phys. Chem.* **2003**, *54*, 141. (b) Shi, Y.; Liu, J.; Yang, Y. *J. Appl. Phys.* **2000**, *87*, 3254. (b) Nguyen, T.-Q.; Martini, I.; Liu, J.; Schwartz, B. J. *J. Phys. Chem. B* **2000**, *104*, 237. (c) Parker, I. D. *J. Appl. Phys.* **1994**, *75*, 1656. (d) Bharathan, J. M.; Yang, Y. *J. Appl. Phys.* **1998**, *84*, 3207. (e) Kim, S. H.; Choi, K. H.; Lee, H. M.; Hwang, D. H.; Do, L. M.; Chu, H. Y.; Zyung, T. *J. Appl. Phys.* **2000**, *87*, 882.

(15) Campbell, I. H.; Hagler, T. W.; Smith, D. L. *Phys. Rev. Lett.* **1996**, *76*, 1900.

(16) (a) Berthier, C.; Gorecki, W.; Minier, M. *Solid State Ionics* **1983**, *11*, 91. (b) Wong, T.; Papke, B. L.; Shriver, D. F.; Brodwin, M. *Solid State Ionics* **1981**, *5*, 689. (c) Ratner, M. A.; Shriver, D. F. *Chem. Rev.* **1988**, *88*, 109. (d) Borodin, O.; Smith, G. D. *Macromolecules* **2006**, *39*, 1620. (e) Müller-Plathe, F.; van Gunsteren, W. F. *J. Chem. Phys.* **1995**, *103*, 4745. (f) Duan, Y.; Halley, J. W. *J. Chem. Phys.* **2005**, *122*, 054702.

(17) (a) Weston, J. E.; Steele, B. C. H. *Solid State Ion.* **1981**, *2*, 347. (b) Bailey, F. E.; Koleske, J. V. *Poly(ethylene oxide)*; Academic: New York, 1976.(c) Weston, J. E.; Steele, B. C. H. *Solid State Ionics* **1982**, *7*, 81. (d) Pearce, R.; Vanco, G. J. *Macromolecules* **1997**, *30*, 5843.

(18) (a) Zen, A.; Pflaum, J.; Hirschmann, S.; Zhuang, W.; Jaiser, F.; Asawapirom, U.; Rabe, J. P.; Scherf, U.; Neher, D. *Adv. Funct. Mater.* **2004**, *14*, 757. (b) McCulloch, I.; Heeney, M.; Bailey, C.; Genevicius, K.; MacDonald, I.; Shkunov, M.; Sparrowe, D.; Tierney, S.; Wagner, R.; Zhang, W.; Chabinyc, M. L.; Kline, R. J.; McGehee, M. D.; Toney, M. F. *Nat. Mater.* **2006**, *5*, 328.

(19) (a) Nguyen, T.-Q.; Doan, V.; Schwartz, B. J. *J. Chem. Phys.* **1999**, *110*, 4068. (b) Yang, H.; Shin, T. J.; Yang, L.; Cho, K.; Ryu, C. Y.; Bao, Z. *Adv. Funct. Mater.* **2005**, *15*, 671.

(20) (a) Magonov, S. N.; Reneker, D. H. *Annu. Rev. Mater. Sci.* **1997**, *27*, 175. (b) O'Neil, K. D.; Semenikhin, O. A. *J. Phys. Chem. C* **2007**, *111*, 14823. (c) Hugger, S.; Thomann, R.; Heinzel, T.; Thurn-Albrecht, T. *Colloid Polym. Sci.* **2004**, *282*, 932. (d) O'Neil, K. D.; Semenikhin, O. A. *J. Phys. Chem. C* **2007**, *111*, 14823. (e) McLean, R. S.; Doyle, M.; Sauer, B. B. *Macromolecules* **2000**, *33*, 6541.

(21) (a) Blom, P. W.; de Jong, M. J. M.; Vleggaar, J. J. M. *Appl. Phys. Lett.* **1996**, *68*, 3308. (b) Bozano, L.; Carter, S. A.; Scott, J. C.; Malliaras, G. G.; Brock, P. J. *Appl. Phys. Lett.* **1999**, *74*, 1132. (c) Mihailetchi, V. D.; van Duren, J. K. J.; Blom, P. W. M.; Hummelen, J. C.; Janssen, R. A. J.; Kroon, J. M.; Rispens, M. T.; Verhees, W. J. H.; Wienk, M. M. *Adv. Funct. Mater.* **2003**, *13*, 43. (d) Kang, H. S.; Kim, K. H.; Kim, M. S.; Park, K. T.; Kim, K. M.; Lee, T. H.; Lee, C. Y.; Joo, J.; Lee, D. W.; Hong, Y. R.; Kim, K.; Lee, G. J.; Jin, J. I. *Synth. Met.* **2002**, *130*, 279. (e) Brütting, W.; Berleb, S.; Mückl, A. G. *Synth. Met.* **2001**, *122*, 99. (f) Khan, M. A.; Xu, W.; ul-Haq, K.; Bai, Y.; Jiang, X. Y.; Zhang, Z. L.; Zhu, Zhang, Z. L.; Zhu, W. Q.; Zhu, W. Q. *J. Appl. Phys.* **2008**, *103*, 014509.

(22) (a) Yu, G.; Cao, Y.; Zhang, C.; Li, Y.; Gao, J.; Heeger, A. J. *Appl. Phys. Lett.* **1998**, *73*, 111. (b) Yang, J.; Pei, Q. *J. Appl. Phys.* **1997**, *81*, 3294. (c) Cao, Y.; Yu, G.; Yang, Y.; Heeger, A. J. *Appl. Phys. Lett.* **1996**, *68*, 3218.

(23) (a) deMello, C. J.; Tessler, N.; Graham, S. C.; Friend, R. H. *Phys. Rev. B* **1998**, *57*, 12951. (b) Ouisse, T.; Stéphan, O.; Armand, M.; Leprêtre, J. C. *J. Appl. Phys.* **2002**, *92*, 2795.

(24) (a) Gu, Z.; Shen, Q. D.; Zhang, J.; Yang, C. Y.; Bao, Y. J. *J. Appl. Polym. Sci.* **2006**, *100*, 2930. (b) Edman, L.; Pauchard, M.; Liu, B.; Bazan, G. C.; Moses, D.; Heeger, A. J. *Appl. Phys. Lett.* **2003**, *82*, 3961. (c) Gu, Z.; Bao, Y. J.; Zhang, Y.; Wang, M.; Shen, Q. D. *Macromolecules* **2006**, *39*, 3125.